Interaction of NaCl with solid water

A. Borodin, O. Höfft, U. Kahnert, and V. Kempter[a)]
Institut für Physik und Physikalische Technologien, Technische Universität Clausthal, Leibnizstrasse 4, D-38678 Clausthal-Zellerfeld, Germany

A. Poddey and P. E. Blöchl
Institut für Theoretische Physik, Technische Universität Clausthal, Leibnizstrasse 10, D-38678 Clausthal-Zellerfeld, Germany

(Received 22 March 2004; accepted 18 August 2004)

The interaction of NaCl with solid water, deposited on tungsten at 80 K, was investigated with metastable impact electron spectroscopy (MIES) and ultraviolet photoelectron spectroscopy (UPS) (He I). We have studied the ionization of Cl($3p$) and the $1b_1$, $3a_1$, and $1b_2$ bands of molecular water. The results are supplemented by first-principles density functional theory (DFT) calculations of the electronic structure of solvated Cl^- ions. We have prepared NaCl/water interfaces at 80 K, NaCl layers on thin films of solid water, and H_2O ad-layers on thin NaCl films; they were annealed between 80 and 300 K. At 80 K, closed layers of NaCl on H_2O, and vice versa, are obtained; no interpenetration of the two components H_2O and NaCl was observed. However, ionic dissociation of NaCl takes place when H_2O and NaCl are in direct contact. Above 115 K solvation of the ionic species Cl^- becomes significant. Our results are compatible with a transition of Cl^- species from an interface site (Cl in direct contact with the NaCl lattice) to an energetically favored configuration, where Cl species are solvated. The DFT calculations show that Cl^- species, surrounded by their solvation shell, are nevertheless by some extent accessed by MIES because the Cl($3p$)-charge cloud extends through the solvation shell. Water desorption is noticeable around 145 K, but is not complete before 170 K, about 15 K higher than for pure solid water. Above 150 K the NaCl-induced modification of the water network gives rise to gas phase like structures in the water spectra. In particular, the $3a_1$ emission turns into a well-defined peak. This suggests that under these conditions water molecules interact mainly with Cl^- rather than among themselves. Above 170 K only Cl is detected on the surface and desorbs around 450 K. © *2004 American Institute of Physics.*
[DOI: 10.1063/1.1805498]

I. INTRODUCTION

The understanding of the interaction of salt molecules with water and vice versa of water molecules with NaCl surfaces, is of interest in various fields, ranging from biological systems to catalysis and environmental sciences. Hydrated NaCl particles extracted from the ocean may become a part of the atmosphere or get deposited on the ocean shore. In both situations they play an important role as providers for chloride species and/or catalysts for pollution reactions involving (N-O)-compounds.[1,2]

In the chemistry of aerosols and clouds the surface layers to be investigated are usually extremely thin. Low-energy reactive ion scattering (RIS) has proven to be a sensitive tool for monitoring surface species.[3] In RIS a low-energy Cs^+ ion beam (3–100 eV) is surface scattered and the scattered ions are mass analyzed. Association products of Cs^+ with neutral species adsorbed at the surface, here water, and, in addition, ions preexisting at the surface are ejected. For NaCl exposed to solid water (SW) at 100 K, RIS showed that NaCl dissociates almost completely, forming Na^+-water complexes.[3] It was concluded that these solvated species do not migrate across one water bilayer of the water film over several minutes.

In the past, electron spectroscopies have been demonstrated to be a powerful tool to study the physics and chemistry on surfaces.[4,5] For insulating substrates the problem of surface charging could be circumvented by working with sufficiently thin films deposited on conducting substrates. In the metastable impact electron spectroscopy (MIES) metastable He atoms with thermal energy interact exclusively with the topmost layer via Auger processes.[6,7] Their probability depends essentially on the overlap between the $1s$ He orbital and those of the outermost surface layer that contribute to the charge density in the toplayer. Thus, the ejected electrons bear information on the electronic structure of the surface top layer. So far, the combination of MIES and ultraviolet photoelectron spectroscopy (UPS) (He I) was applied to the study of the interaction of SW with Na atoms and CH_3OH,[8] of SW with CsCl,[9,10] and, supported by cluster density functional theory (DFT) calculations, to the interaction of Na with CH_3OH.[11,12]

It is the aim of the present work to study details of the solvation process, in particular, its temperature dependence, for NaCl interacting with SW by combining MIES and UPS. Films of SW held at 80 K, were exposed to NaCl, and the change of the electronic structure with the temperature of the

a)FAX: -72-3600; Electronic mail: volker.kempter@tu-clausthal.de

NaCl-exposed film was monitored under the *in situ* control of MIES and UPS. Additional information on the solvation process was obtained from the interaction of water molecules with NaCl films produced at 80 K. The interpretation of the MIES data obtained for Cl^- in aqueous environment required first principles DFT calculations to disentangle the contributions resulting from the ionization of $1b_1$ water and the $Cl(3p)$ orbitals, both contributing to the charge density in the surface toplayer.

All films are grown via *in situ* deposition onto a tungsten substrate. As was pointed out previously, this approach has several advantages: (1) it is a relatively simple matter to investigate both surface and bulk phenomena with the technique combination MIES and UPS,[8] (2) surface charging is eliminated for sufficiently thin films,[8] and (3) condensation of water molecules below about 135 K results in the formation of an amorphous form of SW.[13,14] Its properties are believed to be similar to those of liquid water, in particular, with regard to its molecular orientation, therefore, SW can be considered as a model for liquid water with a very low vapor pressure and, thus, accessible to analysis with surface analytical techniques. This makes a comparison with UPS results on liquid water surfaces and aqueous solutions meaningful.[6,15–17]

II. EXPERIMENTAL AND THEORETICAL METHODS

A. Experimental remarks

Experimental details can be found elsewhere.[18–22] Briefly, the apparatus is equipped with a cold-cathode gas discharge source for the production of metastable $He^*(^3S/^1S)$ ($E^*=19.8/20.6$ eV) atoms with thermal kinetic energy and He I photons ($E^*=21.2$ eV) as a source for ultraviolet photoelectron spectroscopy (UPS). The intensity ratio $^3S/^1S$ is found to be 7:1. Since the metastables approach the surface with near-thermal kinetic energy (60 to 100 meV), this technique is nondestructive and highly surface sensitive (see Refs. 6 and 7 for more detailed introductions into MIES and its various applications in molecular and surface spectroscopy). The spectral contributions from metastables and photons are separated by means of a time-of-flight technique. MIES and UPS spectra were acquired with incident photon/metastable beams 45° with respect to the surface normal; electrons emitted in the direction normal to the surface are analyzed. Collection of a MIES/UPS spectrum requires ≈100 s. The measurements were performed using a hemispherical analyzer. In order to minimize charge-up phenomena, we worked with low beam currents densities, and thus an energy resolution of 600 meV was employed for MIES/UPS. The spectra showed no basic changes at 250 meV resolution. A second photon source is at our disposal providing He I and He II (40.8 eV) photons.

By applying suitable biasing electrons emitted from the Fermi level E_F are registered at 19.8 eV [the potential energy of $He^*(2\,^3S)$]. Consequently, the onset of the spectra at low kinetic (high binding) energies occurs at the work function of the sample. The variation of the onset of the spectra at low kinetic energies with exposure gives then directly the exposure dependence of the surface work function.

The sample can be cooled with LN_2 to 80 K. The temperature, measured with a thermocouple in direct contact with the front of the tungsten single crystal, is estimated to be accurate within ±10 K. The surface was exposed to water by backfilling the chamber. The water was cleaned by several freeze-pump-thaw cycles. The amount of surface-adsorbed water is estimated on the basis of our previous results for the water titania interaction (Ref. 22); essentially, we make use of the fact that (a) water adsorption leads to an initial work function decrease up to half coverage of the surface and (b) the MIES signal from water saturates for full coverage of the surface. From this we conclude that at 2L exposure the surface is covered by one bilayer (BL) of water. At 5L emission from the tungsten substrate has essentially disappeared in the UPS(He I) spectra.

Exposure of NaCl molecules was made by thermal evaporation of polycrystalline material at ≈700 K (for details see Ref. 23). Evaporation of monomers takes place as concluded from the fact that the UPS spectra for adsorption on tungsten in the submonolayer regime resemble closely those of gaseous NaCl molecules.[23] The NaCl exposure is given in units of monolayer equivalents (MLE); at 1 MLE the saturation coverage of the surface would be reached if it would not be for penetration effects. Our previous results for salt adsorption on tungsten indicate that the observed work function minimum occurs at 0.5 MLE.[23–26] For the exposure of NaCl on solid water we assume that the sticking coefficient is the same as on tungsten. Annealing of the prepared films is done stepwise; during the collection of the MIES/UPS spectra the substrate temperature is kept constant.

B. Computational details

We performed density functional theory (DFT) calculations[27,28] using PBE gradient corrections[29] on the electronic structure of a chlorine ion in liquid water. The calculations have been performed using the CP-PAW implementation of the projector augmented wave (PAW) method.[30] We used one projector function and one pair of partial waves per angular momentum (ℓ,m) for the s and p orbitals of chlorine and oxygen, respectively, and two projector functions for the hydrogen s orbital. The plane wave cutoff for the wave functions has been 30 Ry. We used a super cell with lattice constant $a=15$ Å, containing 111 water molecules and one Cl ion, corresponding to the density of liquid water. Our calculations therefore refer to the dilute limit of Cl ions. The slow relaxation times of liquid water mandates large equilibration times before a realistic structure of liquid water is obtained. Therefore, the initial structure for the density functional calculations has been obtained from a classical molecular-dynamics simulation using the TIP3P model[31] for water and a force field consisting of a van der Waals interaction with the water oxygen atoms and an electrostatic interaction with all other atoms in the system for Cl (Ref. 32) (see Table I for the TIP3P parameters). The system has been equilibrated for 0.87 ns between 200 and 300 K, following a heating-cooling cycle lasting about 0.27 ns. From this structure we started a PAW calculation and quenched the structure within 1.15 ps into a nearby local minimum state. In order to analyze the decay of the Cl-related state at the top of the

TABLE I. Parameters used for the force field calculations in Hartree atomic units ($e=\hbar=m_e=4\pi\epsilon_0=1$). The internal structure of the water molecules, defined by the intramolecular distances d(O-H) and d(H-H) are kept rigid. The van der Waals interaction between Cl and O atoms are defined by $V_{dW}=c_{12}r^{-12}-c_6r^{-6}$. In addition the intermolecular electrostatic interaction between the atoms with charges q_H, q_O, and q_{Cl} have been considered.

q_O	−0.834	c_6(O-O)	1.9235	c_{12}(O-O)	143.0775
q_H	0.417	c_6(Cl-O)	1.2745	c_{12}(Cl-O)	101.6710
q_{Cl}	−1	d(O-H)	1.8088	d(H-H)	2.8614

water valence state we projected the three Cl($3p$) states onto the individual water molecules. The projection is such that the one-center expansion at each atom of a molecule is integrated out to a radius which is 1.1 times larger than the covalent radius.[30]

III. RESULTS AND DISCUSSION

This section starts with the discussion of the spectral features expected from the ionization of NaCl and water. In the present paper, we confine ourselves to a qualitative analysis of the MIES spectra: the comparison of the MIES and UPS spectra indicates that the spectral features seen in MIES are due to Auger deexcitation (AD) of He*.[6,7] Here, the potential energy of a surface electron is utilized to eject the $2s$ He electron. In this case, the position of the spectral feature gives the experimental binding energy of the electron emitted. All results are presented as function of the binding energy E_B of the emitted electrons; electrons from the Fermi level would appear at zero energy in the MIES and UPS spectra. Quantitative methods are available to either synthesize MIES spectra[33,34] (see Ref. 35 for an example) or for their deconvolution.[6] For a qualitative analysis of the present data we suppose that the intensity of the spectral features from the AD process reflects directly the density of states initially populated. Thus, we compare the MIES results directly with the DFT-density of states (DOS) (Sec. III B). In contrast, the UPS results depend upon both the DOS of the initial and final states involved in the photoionization process.

A. Signature of NaCl and water species in MIES and UPS

Water exposure produces the three features $1b_1$, $3a_1$, and $1b_2$ seen in MIES and UPS as well as in the DOS of the water film (for previous studies on SW with MIES/UPS see Refs. 8 and 22). It should be noted that the UPS data for SW films are rather similar to those for liquid water.[15] According to the first-principles calculations carried out on ice in Ref. 36, the $1b_2$ peak represents bonding orbitals between O and H atoms in the water molecule. The $3a_1$ peak is attributed to the in-plane O($2p$) orbital. The $1b_1$ peak represents the O($2p$) orbital perpendicular to the plane of the water molecule. The $3a_1$ feature (considerably more diffuse than $1b_1$ and $1b_2$) corresponds to delocalized states with intermolecular contributions from different water molecules interacting via hydrogen bonds. Apparently, the broad $3a_1$ feature is characteristic for condensed water, either in the liquid or solid phase, and signals the presence of a water network, formed by hydrogen bonds (see also Sec. III B).

Combined MIES/UPS results for alkali halide films on tungsten are available for NaCl,[23,37] CsI,[24] and LiF.[25,26] The Na species cannot be detected directly with our techniques because Na is present as ionic species; $3s$ Na is empty, and, thus, not accessible to UPS and MIES. The available potential energy of the He I photons and the metastable He atoms is not sufficient to ionize the Na $2p$ shell. The energetic position of the Cl($3p$) emission seen in the present work agrees well with literature. The overall similarity of the MIES and UPS(He I) spectra suggests that the MIES spectra are due to the AD process. In general, the transition $Cl^-(3p^6) \rightarrow Cl^0(3p^5)$ displays a "fine structure" that can give information on the chemical environment of the chloride species. The fine structure splitting of the transition $Cl^-(3p^6) \rightarrow Cl^0(3p^5;{}^2P_{3/2;1/2})$ in the free Cl^- ion is 0.11 eV,[38] too small to be observed in the present work. The free NaCl molecule displays a ($^2\Sigma$-$^2\Pi$) Stark splitting of 0.46 eV in UPS,[36] originating from the strong axial field in the NaCl molecule. The spectra of solid NaCl, films, or single crystals, between 5 and 10 eV originate from the ionization of the Cl($3p$) states of the valence band, and show a "double-peak" structure that reflects the valence band density of the states.[39,40] The peak separation is 0.9 eV in the He II spectra.[37] Our UPS(He I) spectra also show this splitting. On the other hand, the MIES spectra from NaCl films do not display this splitting instead, a single peak is found that is asymmetric towards larger binding energies (Refs. 23 and 37 and present work).

Solvated Cl^- species can be expected to experience an essentially isotropic environment. Therefore, the situation will resemble that of a free ion, and a single peak can be expected from the $Cl^-(3p^6) \rightarrow Cl^0(3p^5)$ transition (apart from the small fine structure splitting which cannot be resolved). On the other hand, the UPS spectra from solvated molecular NaCl species would show the ($^2\Sigma$-$^2\Pi$) Stark splitting of 0.46 eV. Finally, for NaCl films on SW the UPS spectra should display the double-peak structure of the Cl($3p$) valence band emission, provided that the film has solid state properties, expected for more than two NaCl layers.[23] In summary, the shape of the Cl($3p$) emission, in particular, in the UPS spectra, will provide information on the chemical identity of the adsorbed species and on its molecular or dissociative adsorption.

Although we have applied UPS with He II radiation to $NaCl/H_2O$, these results are not presented here: the low efficiency for Cl($3p$) ionization by He II makes a separation of the contributions $1b_1$ and Cl($3p$) between 5 and 6 eV difficult.

B. Electronic structure of solvated Cl^- species

The DFT calculations reproduce the characteristic three-peak structure of the oxygen p band (Fig. 1). The three peak structure corresponds to the antisymmetric O-H bonds ($1b_2$), the symmetric O-H bonds ($3a_1$) with the p orbital lying in both mirror planes of the water molecule, and the p

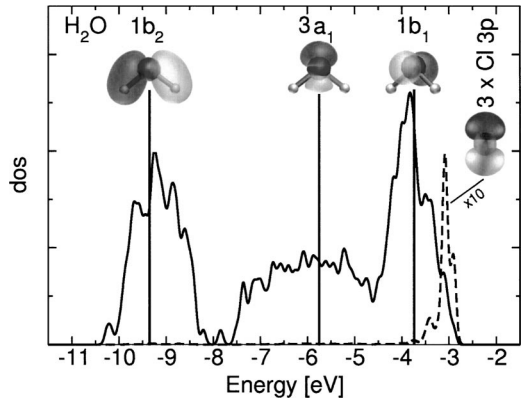

FIG. 1. Density of states of a Cl ion solvated in water. The density of states projected onto Cl($3p$) shown as dashed line is magnified by a factor of 10. The vertical lines correspond to the states of an isolated water molecule, shifted globally, so that the center of the oxygen p band align with that of the bulk water.

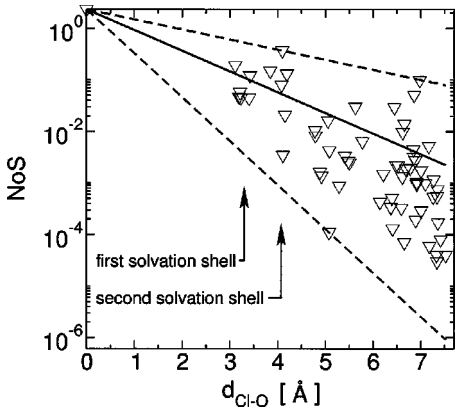

FIG. 3. Decay of the Cl($3p$) states in water. Logarithmic plot of the water-projected number of states of those three states with predominant Cl($3p$)-character. This weight decays with a factor of 0.4 ± 0.25 for every angstrom distance from the Cl atom. The Cl-O distances for the first solvation shell lie between 3.12 and 3.42 Å. The oxygen atoms of the water molecules in the second solvation shell are found between 3.84 and 4.15 Å. See text for further details.

orbital oriented perpendicular to the bond plane ($1b_1$). The peak of the $2s$ O-band lies well separated below the p band.

There has been a discussion about the origin of the wide broadening of the $3a_1$ band as compared to the $1b_1$ and $1b_2$ bands.[36] We investigated if this broadening can be related to structural changes or to the hydrogen bond network. For that purpose we randomly selected five water molecules, and compared their density of states, once in bulk water and secondly as isolated molecules in the same geometry as in the bulk cell (Fig. 2). The broadening of $3a_1$ band in the solid is substantially larger than for the other two. We clearly see that this broadening is due to the coupling with the neighboring water molecules, and not to intramolecular structural distortions, because the width of the $3a_1$ states in isolation is comparable to that of the other two bands. We attribute the particularly large broadening of the $3a_1$ band to the nature of the contributing states, which can couple to the neighboring water molecules both via the hydrogen atoms and via the oxygen lone pair. The $1b_1$ and $1b_2$ states, on the other hand, can only couple either via the hydrogen atoms ($1b_2$) or via the oxygen p orbitals ($1b_1$). Thus, the $3a_1$ state is in the best position to form delocalized wave functions that extend over many water molecules, which is the origin for the width of the $3a_1$ band.

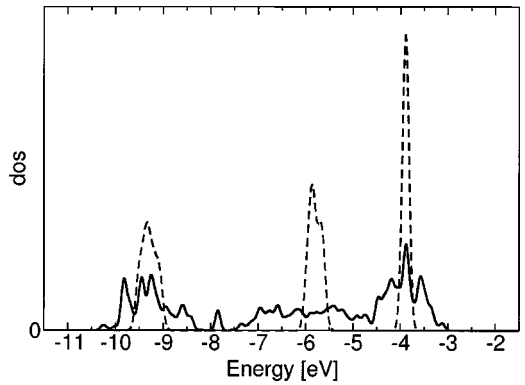

FIG. 2. Sum of the density of states of five randomly selected water molecules, once in bulk water (full line) and secondly as isolated molecules in the same intramolecular geometry as in the bulk cell (dashed line). See text for further details.

The Cl($3p$) states form a rather narrow band located at the top of the valence band of the water molecules. Although these states are fairly localized on the Cl atoms, the tails of the wave function extend over several water molecules into the solvation shell. They couple nearly exclusively to the $1b_1$ orbitals of the neighboring water molecules. This is because the Cl($3p$) orbitals hybridize predominantly with those states of the solvent that are energetically close.

Our main interest was to quantify the decay of the Cl state into the bulk of the water. This will provide a measure for the relative intensities of the MIES spectra from the Cl ions depending on its position at the surface or in the subsurface. He* metastables interact only with the tails of the wave function of the outermost surface atoms. The wave functions attributed to the Cl atoms extend to the surface and contribute approximately proportional to their weight to the surface atoms. We evaluated the weight of the three wave functions with predominantly Cl($3p$) character, which are located within an energy window of width <0.2 eV at the top of the upper occupied band of water, on the water molecules, shown in Fig. 3. We find a decay corresponding to a factor $0.4(\pm0.25)$ Å^{-1} distance from the Cl atom. The decay has been obtained from a fit of $W_{\mathrm{Cl}}e^{-\lambda r}$, where W_{Cl} is the weight of the states on the Cl atom (full line). The dashed lines correspond to the maximum and minimum values of λ obtained from individual data points. The position of the oxygen atom has been used to calculate the distance from the Cl atom. The wide spread stems from the inhomogeneous coupling of the Cl($3p$) orbitals along the hydrogen bond network.

Interestingly, the largest weight is not found on the first, but on the second solvation shell. The electron on the Cl atom couples to the high-lying $1b_1$ orbitals. The lobes of the latter orbitals point perpendicular to the hydrogen bonds. This implies that the $1b_1$ orbitals on the molecules in the first

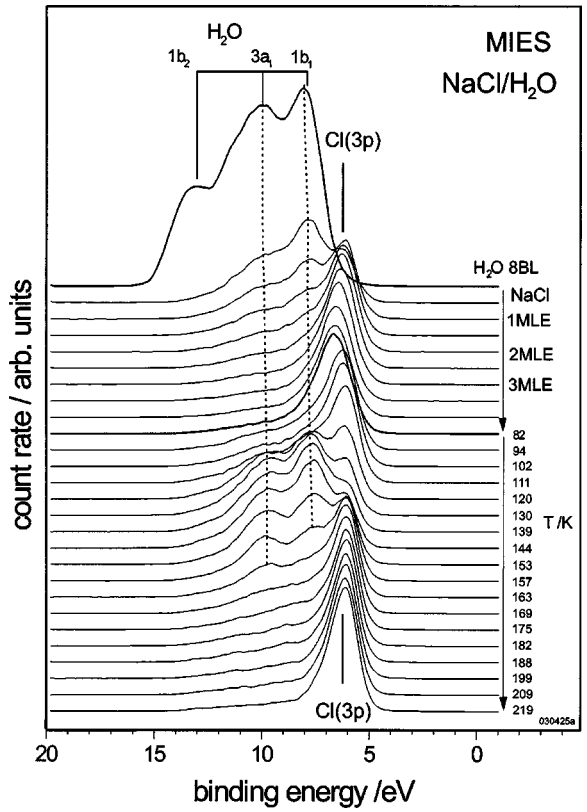

FIG. 4. MIES spectra for solid H_2O (3BL) on tungsten kept at 80 K (top spectrum), and for NaCl exposure of the H_2O film. Lower part: spectra obtained during annealing of the NaCl exposed film (80 to 210 K).

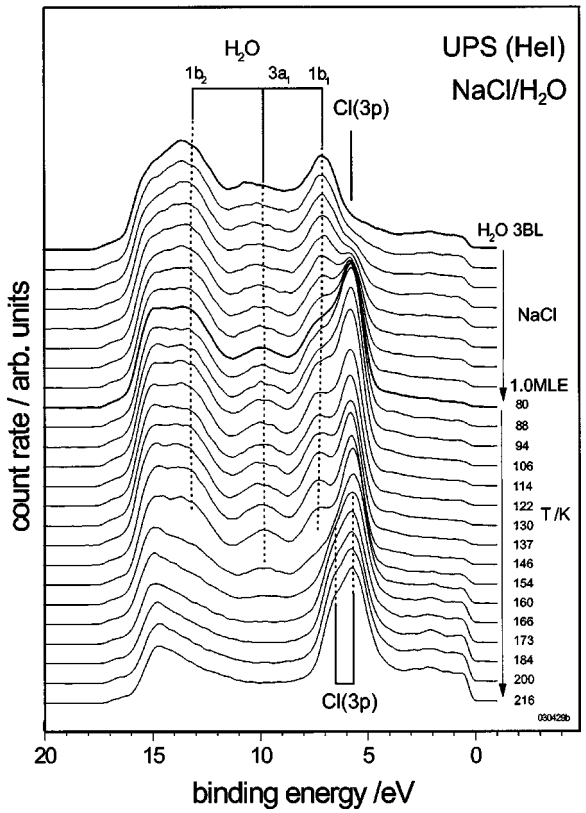

FIG. 5. As Fig. 4, but UPS(He I) spectra.

solvation shell are oriented unfavorably for an efficient coupling to the Cl orbitals. As the water molecules in the second shell do not have this orientational relationship, the Cl($3p$) orbitals can extend more efficiently into $1b_1$ states of the water molecules in the second shell.

The first solvation shell consists of six water molecules. The H-bonds to the first solvation shell range from 2.17 to 2.63 Å. The next Cl-H distance lies well separated by 3.19 Å. Our finding differs from previous calculations at finite temperatures that obtain a solvation shell of five molecules.[41] We attribute this difference to the fact that our structure is obtained from a quench into the ground state. At this point we cannot exclude that, due to the rapid quenching, our calculation still reflects some structural features of the TIP3P model.

C. Interaction at NaCl-water interfaces

Figures 4 and 5 summarize the MIES and UPS results obtained for a film of SW, held at 82 K (abbreviated by $NaCl/H_2O$), during its exposure to NaCl followed by film heating to 210 K. The top spectrum of Fig. 4 is for SW (8BL) (BL: bilayer). The following nine spectra display the changes occurring during the exposure of 4MLE NaCl. A shoulder develops at the right side of $1b_1$ and turns into the peak denoted by Cl($3p$), identified as emission from the Cl($3p$) orbital. Apparently, a closed NaCl layer can be produced on SW at this temperature (10th spectrum from top). This was not possible for CsCl at 130 K where a mixed layer formed, consisting of H_2O, Cs, and Cl species.[9,10] When heating beyond 110 K, the spectral features of water reappear gradually, and become the dominant structures in the spectra between 120 and 140 K. Clearly, water species penetrate deep enough into the NaCl toplayer to become accessible to MIES. Around 145 K water desorption becomes significant as signaled by the renewed rise of Cl($3p$), concurrent with the decrease of the water features; around 170 K, according to MIES, all water has desorbed, and Cl($3p$) is seen only. Auxiliary experiments carried out for SW on tungsten show that the water desorption in that case is completed about 20 K earlier than for $NaCl/H_2O$.

Additional information on the first step of the NaCl interaction with SW comes from the He I results of Fig. 5. The top spectrum is for water (3BL) on tungsten. Besides the emission from the water states $1b_1$, $3a_1$, and $1b_2$, contributions from the tungsten substrate can be noticed between the Fermi level ($E_B=0$ eV) and $E_B=5$ eV. The Cl($3p$) feature is seen as a single, sharp peak at $E_B=5.6$ eV, its shoulder towards larger binding energies is clearly due to $1b_1$ water emission. When most of the water has desorbed ($T>166$ K), Cl($3p$) develops the double-peak structure typical for the NaCl bulk, here for NaCl film formation on the W substrate. As outlined in Sec. III A, the sharp Cl($3p$) peak found in aqueous environment can be considered as evidence for ionic dissociation during NaCl adsorption. Apparently, on SW the resulting species Cl^- and Na^+ adsorb independently without much mutual lateral interaction. This is in full accord with the findings of RIS where dissociative adsorption of NaCl on SW, followed by the formation of Na^+-water clus-

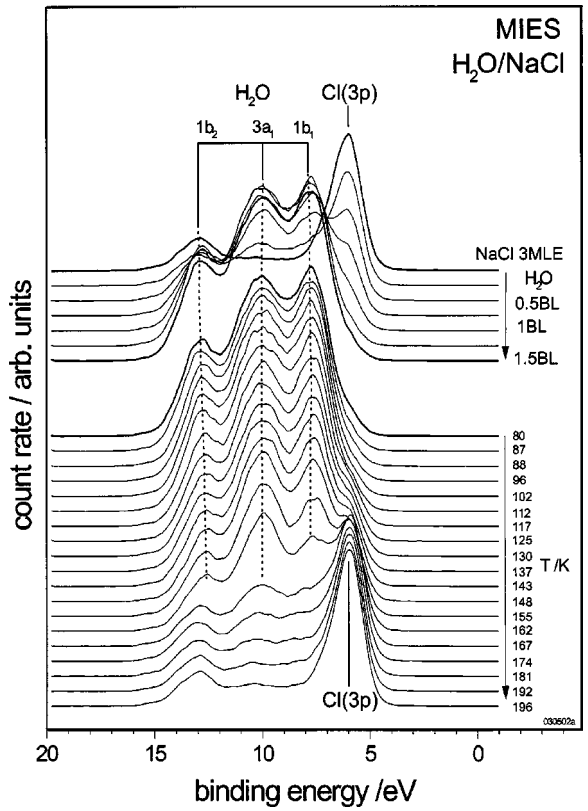

FIG. 6. MIES spectra for a NaCl film (3MLE) on tungsten kept at 80 K (top spectrum), and during H_2O exposure (1BL) of the NaCl film. Lower part: spectra obtained during annealing of the H_2O-exposed NaCl film (80 to 210 K).

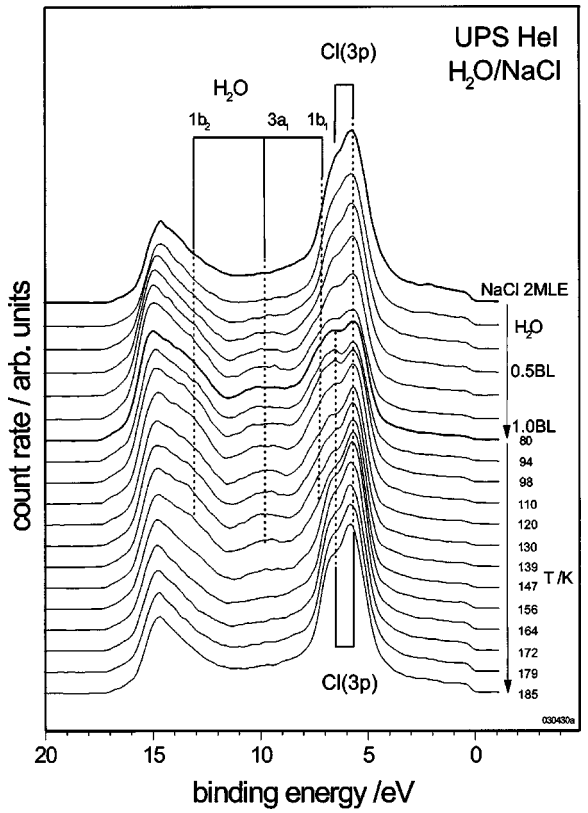

FIG. 7. As Fig. 6, but UPS(He I) spectra.

ters, was found at 100 K.[3] Support for cluster formation comes also from the study of the ions emitted during ESD from NaCl and water, coadsorbed on a condensed Ar substrate (35 K).[42] It was demonstrated that solvated Na^+ ions, $Na^+(H_2O)_n$ $(n=1-4)$, desorbed more intensively than bare Na^+ ions.

Figures 6 and 7 summarize the results collected for water films deposited on NaCl films at 80 K (abbreviated by H_2O/NaCl). We find that the exposure required for a closed layer is comparable to that required on tungsten. Therefore, water penetration into the NaCl film does not take place at 80 K. The MIES data obtained during the annealing to 300 K reveal that above 105 K both species H_2O and Cl are seen with MIES, even if at 80 K, as in Fig. 6, practically only H_2O species were present in the outermost layer. The He I results also demonstrate that Cl$(3p)$ becomes more pronounced as a consequence of the annealing, and, thus, Cl species must become located closer to the surface. While Cl$(3p)$ is a sharp peak in aqueous environment, the double-peak structure of the NaCl bulk develops when the water desorbs.

Figure 8 displays the intensities of $H_2O(1b_1)$ and Cl$(3p)$, extracted from the MIES data, versus the annealing temperature. In the case of NaCl/H_2O the rise of $1b_1$ above 105 K is correlated with a decrease of Cl$(3p)$. Clearly, water species are now present in the top layer. On the other hand, for H_2O/NaCl the rise of Cl$(3p)$ is correlated with a decrease of $1b_1$ in the same temperature range. Above 145 K the temperature dependence of the signals is the same for both NaCl/H_2O and H_2O/NaCl. This suggests that the composition of the top layer is the same. The Cl$(3p)$ intensity present at 140 K, shortly before water desorption becomes significant, does not necessarily imply that the shielding of the Cl^- species by water is incomplete. Instead,

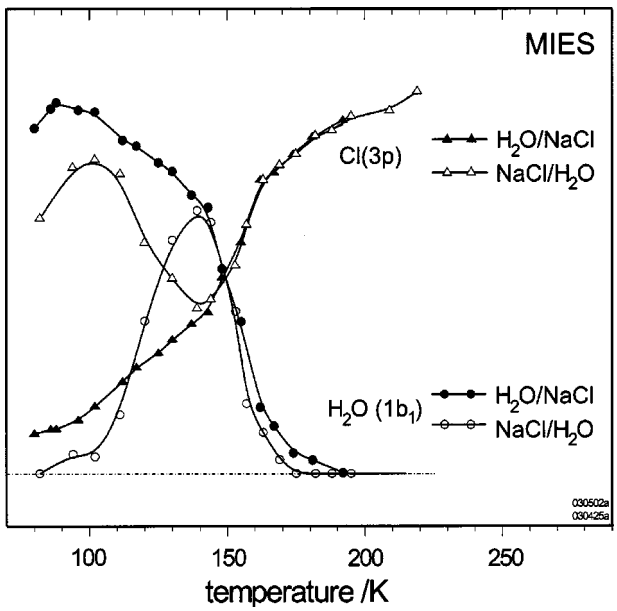

FIG. 8. Intensities of $1b_1$ of H_2O and Cl$(3p)$ from Cl^- as a function of the annealing temperature (80 to 210 K) for (a) NaCl(1MLE)/H_2O(3BL) and (b) H_2O(1BL)/NaCl(3MLE). Data from the MIES spectra of Figs. 4 and 6.

Cl($3p$)-charge density may extend through the solvation shell, rendering the solvated Cl^- species accessible to MIES. This viewpoint is supported by two observations given below.

(1) Mixed NaCl/water films produced by codeposition of the two components at 80 K on tungsten (not shown) also display a shoulder identified as $1b_1$ which in shape and intensity resembles that seen in Figs. 4 and 5 at annealing temperatures above 120 K.

(2) As far as Fig. 4 is concerned, the result most relevant from our first-principles calculations on Cl^- species in bulk water (Sec. III B), is the penetration of the charge density with Cl($3p$) character through the first solvation shell. The projected DOS reproduces qualitatively the MIES spectra in the region between 5 and 10 eV binding energy both in relative position and shape of the spectral features. The calculations indicate, that the residual Cl($3p$) intensity seen around 140 K (before water desorption becomes significant), does not necessarily imply incomplete Cl solvation. The intensity of the wave function beyond the solvation shell may even be higher than that on the solvation shell. The decay of the wave function is, however, strongly anisotropic, and the angular average is most relevant. From the calculations we obtain an average decay of the wave function from Cl to a water molecule of the first solvation shell by a factor of 0.036. The factor from Cl to a water of the second solvation shell is 0.045.

Thus, the first-principles results displayed in Fig. 3 support that a substantial contribution of the Cl($3p$) band is accessed by MIES, even if the Cl ion is fully solvated and located one or two layers beneath the surface of the $NaCl/H_2O$ film. Under these conditions, MIES would detect the charge density extending into the vacuum, consisting of the Cl($3p$) charge density leaking via intermediate water molecules through the solvation shell. A drop of the intensity to about few percent up to few tens percent seems compatible with the calculated scenario.

A scenario for the interaction at interfaces between NaCl and water will now be discussed on the basis of a qualitative free energy profile for the $Cl^-(Na^+)$/ice film interaction. So far, free energy profiles appear to be available only for $Na^+(Cl^-)$ adsorption at the water/NaCl crystal interface.[43] The profile of Fig. 9 presents the change $\Delta F(z)$ of the free energy $F(z)$ felt by the $Cl^-(Na^+)$ ion with respect to the vacuum. It possesses two minima, one for adsorption at a ''surface'' site, denoted by S_1, and another, denoted by S_2, for adsorption at a ''solvent-separated'' site; it was found that the ions are more stably adsorbed under solvent-separated conditions, i.e., as fully solvated species.[43] As discussed for HCl/ice,[44] the details of $\Delta F(z)$ will depend on temperature because of the decrease of the entropic contribution with rising temperature. No significant intermixing of the species takes place at the interface as long as the temperature stays below about 105 K. However, already at 80 K there is strong interaction between NaCl and water species at the interface: the NaCl species become dissociated ionically, as already concluded from RIS results obtained at 100 K.[3] In our work the dissociation is suggested by the peculiar shape of the Cl($3p$) emission in UPS under conditions where NaCl is in

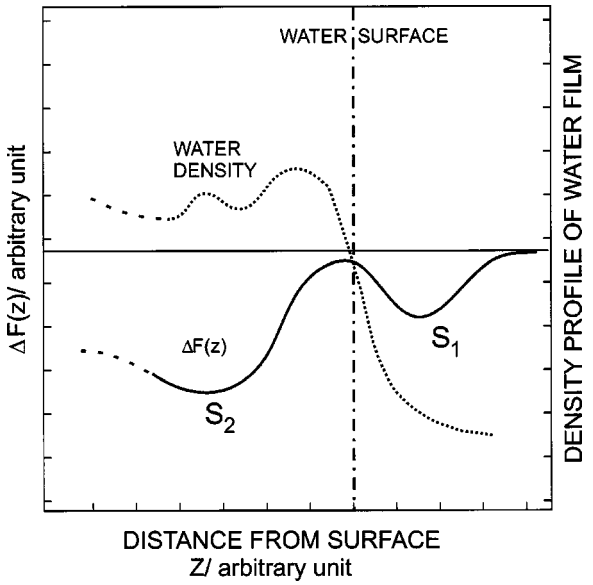

FIG. 9. Qualitative free energy profile $\Delta F(z)$ vs the $Cl^-(Na^+)$ distance from the water surface. The dashed curve refers to the density profile of the water film.

close contact with water. As demonstrated by RIS, Na^+-water) complexes are formed at the interface. With respect to Fig. 9 the adsorbed ions occupy site S_1 up to about 110 K. Above 115 K the mobility of the water molecules is sufficiently enhanced for the transition $S_1 \rightarrow S_2$ to take place, i.e., the Cl^- ions become embedded into the water film, completing their solvation shell. The reason may be that around 110 K, as a consequence of the increase in disorder of the water film, the barrier between S_1 and S_2 has become greatly reduced or has even disappeared, similar to what has been found for HCl/ice.[44] The transition $S_1 \rightarrow S_2$ appears to be related to the amorphous/crystalline transition seen in pure water (135 K) as consequence of the increased water mobility.[13,14]

For H_2O/NaCl we see a decrease of $1b_1$ above 105 K, accompanied by a rise of Cl($3p$). This indicates that Cl^- species become accessible to MIES. This does not necessarily imply that Cl becomes part of the top layer, but rather that the Cl species are located sufficiently close to it so that, as suggested by our DFT results, MIES can detect the Cl($3p$) charge density extending through the respective solvation shell. Following Ref. 43, this can be interpreted as the transition of Cl^- from a site at the H_2O-NaCl interface (''direct'' adsorption) to an energetically more favorable, ''water-separated'' site where the Cl^- species is fully solvated.

Water desorption becomes sizeable above 140 K because feature Cl($3p$) increases, and, at the same time $1b_1$ decreases. On the other hand, desorption is not complete before about 170 K. The MIES spectra of water in the range between 140 and 170 K are gas-phase like, featuring well-defined peaks. This applies in particular to the $3a_1$ emission which was unstructured and diffuse for condensed water.[9,10,36] This indicates that, at this stage, the water emission originates from water species that are no longer involved in a H-bonded water network, but are stabilized by their electrostatic interaction with the salt ions. Conse-

quently, the $3a_1$ hybridization becomes less important, and the $3a_1$ structure becomes sharper.

IV. SUMMARY

We have shown that MIES, in combination with UPS(He I), can be employed successfully to investigate processes between salt molecules (NaCl) and solid water. We have prepared NaCl/water interfaces at 80 K namely NaCl layers on thin films of solid water and water adlayers on thin NaCl films; they were annealed between 80 and 300 K. All experiments were carried out under *in situ* control of MIES and UPS. The spectroscopy results are backed up by first-principles DFT calculations concentrating on the electronic structure of solvated Cl^- ions; the DFT-DOS is compared with the MIES spectra caused by the auger deexcitation process. The following scenario describes our results consistently: at 80 K there is no interpenetration of the two components water and NaCl; however, ionic dissociation of NaCl takes place when water and NaCl are in direct contact. Above 110 K the solvation of the ionic species Cl^- and Na^+ becomes significant. The DFT calculations suggest that Cl^- species which are surrounded by their solvation shell are to some extent accessed by MIES because the $Cl(3p)$-charge cloud extends through the solvation shell. The desorption of water from the mixed film takes place between 145 and 170 K those water species bound ionically to Na^+ and Cl^- are removed last.

ACKNOWLEDGMENTS

Discussions of various aspects of this work with P. Hoang (Besançon) and C. Toubin (Lille) are acknowledged.

[1] A. R. Ravishankara, Science **276**, 1058 (1997).
[2] E. E. Gard, M. J. Kleeman, D. S. Gross *et al.*, Science **279**, 1184 (1998).
[3] S.-C. Park, T. Pradeep, and H. Kang, J. Chem. Phys. **113**, 9373 (2000).
[4] V. E. Henrich and P. A. Cox, *The Surface Science of Metal Oxides* (Cambridge University Press, Cambridge, 1994).
[5] G. Ertl and J. Küppers, *Low Energy Electrons and Surface Chemistry* (VCH, Weinheim, 1985).
[6] H. Morgner, Adv. At., Mol., Opt. Phys. **42**, 387 (2000).
[7] Y. Harada, S. Masuda, and H. Osaki, Chem. Rev. (Washington, D.C.) **97**, 1897 (1997).
[8] J. Günster, S. Krischok, V. Kempter, J. Stultz, and D. W. Goodman, Surf. Rev. Lett. **9**, 1511 (2002).
[9] A. Borodin, O. Höfft, S. Krischok, and V. Kempter, Nucl. Instrum. Methods Phys. Res. B **203**, 205 (2003).
[10] A. Borodin, O. Höfft, S. Krischok, and V. Kempter, J. Phys. Chem. B **107**, 9357 (2003).
[11] A. Borodin, O. Höfft, U. Kahnert, V. Kempter, Y. Ferro, and A. Allouche, J. Chem. Phys. **120**, 8692 (2004).
[12] Y. Ferro, A. Allouche, and V. Kempter, J. Chem. Phys. **120**, 8683 (2004).
[13] J. D. Graham and J. T. Roberts, J. Phys. Chem. **98**, 5974 (1994).
[14] J. P. Devlin, Int. Rev. Phys. Chem. **9**, 29 (1990).
[15] M. Faubel, in *Photoionization and Photodetachment, Part I*, edited by C. Y. Ng (World Scientific, Singapore, 2000), p. 634.
[16] R. Böhm, H. Morgner, J. Overbrodhage, and M. Wulf, Surf. Sci. **317**, 407 (1994).
[17] J. Dietter and H. Morgner, Chem. Phys. **220**, 261 (1997).
[18] W. Maus-Friedrichs, M. Wehrhahn, S. Dieckhoff, and V. Kempter, Surf. Sci. **249**, 149 (1991).
[19] D. Ochs, W. Maus-Friedrichs, M. Brause *et al.*, Surf. Sci. **365**, 557 (1996).
[20] D. Ochs, M. Brause, B. Braun, W. Maus-Friedrichs, and V. Kempter, Surf. Sci. **397**, 101 (1998).
[21] D. Ochs, B. Braun, W. Maus-Friedrichs, and V. Kempter, Surf. Sci. **417**, 390 (1998).
[22] S. Krischok, O. Höfft, J. Günster, J. Stultz, D. W. Goodman, and V. Kempter, Surf. Sci. **495**, 8 (2001).
[23] S. Dieckhoff, H. Müller, H. Brenten, W. Maus-Friedrichs, and V. Kempter, Surf. Sci. **279**, 233 (1992).
[24] A. Hitzke, S. Pülm, H. Müller, R. Hausmann, J. Günster, S. Dieckhoff, W. Maus-Friedrichs, and V. Kempter, Surf. Sci. **291**, 67 (1993).
[25] S. Pülm, A. Hitzke, J. Günster, H. Müller, and V. Kempter, Radiat. Eff. Defects Solids **128**, 151 (1994).
[26] D. Ochs, M. Brause, P. Stracke *et al.*, Surf. Sci. **383**, 162 (1997).
[27] P. Hohenberg and W. Kohn, Phys. Rev. **136**, B864 (1964).
[28] W. Kohn and L. J. Sham, Phys. Rev. **140**, A1133 (1965).
[29] J. P. Perdew, K. Burke, and M. Ernzerhof, Phys. Rev. Lett. **77**, 3865 (1996).
[30] P. E. Blöchl, Phys. Rev. B **50**, 17953 (1994).
[31] W. L. Jorgensen, J. Chandrasekhar, J. D. Madura, R. W. Impey, and M. L. Klein, J. Chem. Phys. **79**, 926 (1983).
[32] M. Patra and M. Karttunen, arXiv:physics/0211059 v2 2003.
[33] P. Eeken, J. M. Fluit, A. Niehaus, and I. Urazgil'din, Surf. Sci. **273**, 160 (1992).
[34] L. N. Kantorovich, A. L. Shluger, P. V. Sushko, J. Günster, P. Stracke, D. W. Goodman, and V. Kempter, Faraday Discuss. **114**, 173 (1999).
[35] M. Brause, S. Skordas, and V. Kempter, Surf. Sci. **445**, 224 (2000).
[36] S. Casassa, P. Ugliengo, and C. Pisani, J. Chem. Phys. **106**, 8030 (1997).
[37] T. Munakata, T. Hirooka, and K. Kuchitsu, J. Electron Spectrosc. Relat. Phenom. **18**, 51 (1980).
[38] W. C. Price, in *Electron Spectroscopy: Theory, Techniques and Applications*, edited by C. R. Brundle and A. D. Baker (Academic, New York, 1977), Vol. 1.
[39] T. Poole, J. G. Jenkins, J. Liesegang, and C. G. Leckey, Phys. Rev. B **11**, 5179 (1975).
[40] N. O. Lipari and A. B. Kunz, Phys. Rev. B **3**, 491 (1971).
[41] J. M. Heuft and E. J. Meijer, J. Chem. Phys. **119**, 11788 (2003).
[42] R. Souda, Phys. Rev. B **65**, 245419 (2002).
[43] H. Shinto, T. Sakakibara, and K. Higashitani, J. Chem. Eng. Jpn. **31**, 771 (1998).
[44] C. Toubin, S. Picaud, P. N. M. Hoang, C. Girardet, R. M. Lynden-Bell, and J. T. Hynes, J. Chem. Phys. **118**, 9814 (2003).